

# Numerical Model of the Insertion Loss Promoted by the Enclosure of a Sound Source

Gil F. Greco<sup>\*1</sup>, Bernardo H. Murta<sup>1</sup>, Iam H. Souza<sup>1</sup>, Tiago B. Romero<sup>1</sup>, Paulo H. Mareze<sup>1</sup>, Arcanjo Lenzi<sup>2</sup> and Júlio A. Cordioli<sup>2</sup>.

1. Undergraduate Program in Acoustical Engineering, Federal University of Santa Maria, RS, Brazil
2. Laboratory of Vibrations and Acoustics, Federal University of Santa Catarina, SC, Brazil

\*Corresponding author: Av. Roraima 1000, Santa Maria, RS, Brasil. 97105-900, gil.greco@eac.ufsm.br

**Abstract:** Usually, the enclosure of a sound source is employed in order to control the noise radiated by industrial machines. This structure changes the path of sound transmission between the sound source and the receiver, imposing a high impedance to the wave propagation. However, the enclosure design requires attention since the enclosure and its panel's vibrational modes will influence its performance. Furthermore, the enclosure's structure response and the acoustic field must be correctly coupled. Although there are models to assess the acoustic performance of enclosures, the multiphysics nature of the problem makes its analytical modeling unfeasible in practice. Thus, this study aims to develop and validate a finite element numerical model to represent the Insertion Loss (IL) promoted by the enclosure of a sound source. For the validation, a enclosure prototype was built in wood and the IL was measured in laboratory. The idea is to develop an efficient numerical model that would be suitable for enclosure's design and optimization.

**Key-words:** Noise Control, Enclosure Design, Acoustic-Structure Interaction, Vibroacoustics.

## 1. Introduction

Usually, it is desirable to control the sound radiation of a certain device, however, most of the times there is no possibilities to modify the constructive characteristics of a sound source. In this cases, enclosing the sound source may be a convenient way to promote a proper sound insulation. In fact, Randall [1], states that the use of a enclosure is the most practical solution when the required noise level reduction is greater than 10 dB. This approach modifies the sound transmission path between the sound source and the receiver, imposing a large impedance to the propagation of the sound wave [2]. Thus, it can be

used to control the noise radiated by machines or noisy devices such as compressors, gears and motors, among others industrial devices.

Although there are models to assess the acoustic performance of enclosures [3,4], the multiphysics nature of the problem makes its analytical modeling unfeasible in practice. Several aspects must be taken into account when designing an enclosure. First, the need of a good accessibility to the sound source can be a drawback since it requires apertures in the enclosure, fact that could allow sound leakage through it. Furthermore, the enclosure's structure will accommodate acoustic modes in the air volume within it, which will increase the intensity of some spectral components of the noise transmitted by the source. These modes can be avoided by the optimization of the geometry of the enclosure as well as through the use of sound absorbent materials inside the enclosure's walls.

Another key point is the vibroacoustic response of the enclosure structure itself. In certain wavelengths, the structure will accommodate vibrational modes whose will reduce substantially the sound insulation in their resonance frequencies. Taking all these facts in mind, the correct coupling between the enclosure's structural response and the acoustical field must be done to allow the development of a representative numerical model of this situation. This coupled analysis is widely studied and modeled by several authors [5,6,7] using the Finite Element (FE) method.

This study goal is to develop and validate a finite element numerical model to represent the Insertion Loss (IL) promoted by the enclosure of a sound source. According to Blanks [2], the efficiency of an enclosure can be better represented by the insertion loss (IL), which quantifies the decrease in the sound power radiated due to insertion of the enclosure over the acoustic source. For the validation, one simple

enclosure prototype was built in only one material, wood (Brazilian ipe) and the sound power was measured in according to ISO 3741 [8]. Further details about the experimental characterization of the problem are exposed in Section 2. The computational models implementations are fully explained in Section 3. The results are discussed in Section 4, while Section 5 presents the conclusions and final considerations about this study.

## 2. Experimental Characterization

According to ISO 3741, the measurement of sound intensity in a surface over the sound source can be done to derive its sound power level. This procedure is done by measuring the sound intensity, emitted by a spherical shaped source with one speaker playing white noise, in 72 isotropic points positioned in a cubical grid of 1 m<sup>3</sup>. The measurements were carried in a reverberant chamber using type-1 hardware. In order to soften reflections from the chamber's walls, 5 square meters of sound absorbing material was added on the walls. According to the theory, this measurement can be conducted in ordinary rooms since it extracts the intensity and radiated power from the enclosed grid points. The Sound Power ( $W$ ) can be derived from the summation of the normal surface intensity magnitude, times the surface segment area of the associated "i" point of the grid:

$$W = \int \vec{I} \cdot d\vec{S} = \sum_{i=1}^N \vec{I}_i \cdot \Delta\vec{S}_i. \quad (1)$$

The frequency dependent Sound Intensity, in  $W/m^2$ , can be derived using a  $p$ - $p$  probe by [9]:

$$I(\omega) = \frac{-1}{\omega \rho_0 \Delta r} \text{Im}[S_{12}(\omega)], \quad (2)$$

where  $\omega$  is the angular frequency,  $\Delta r = 12$  mm is the microphone spacing and  $S_{12}$  is the cross power spectrum of the pressure signal from the mics 1 and 2. Thus, the Sound Power Level ( $L_w$ ) is given by:

$$L_w = 10 \log_{10} \left( \frac{W}{W_{ref}} \right), \quad (3)$$

where  $W_{ref} = 10^{-12}$  W, is the reference power.

In order to derive the insertion loss of a real enclosure, a rectangular box (32 cm x 22 cm x 26.5 cm) with 5 fixed sides and opened at the bottom, was built in a Brazilian species of dry hardwood. All walls have the same thickness ( $d = 24$  mm). The same measurement procedure was repeated with the enclosed source, deriving the spectral sound power level with the enclosure's attenuation. The difference between both results is the IL of the prototype, and was used to validate the FE model.

The experimental sound source, shown in Figure 1, is a spherical speaker with acoustic frequency response range of 80 Hz to 20 kHz, electrical impedance of 8 ohm and diameter of 12 cm.



Figure 1. Experimental Sound Source.

The experimental wood enclosure inside of grid surface during the measurement is in Figure 2.



Figure 2. Sound Power Measurement Using 72 Points of Intensity Data.

## 3. Computational Model

The problem was modeled using two different approaches. First, the Pressure Acoustics, Frequency Domain interface was used to model the sound source, over a finite circular baffle, radiating in a free field condition. The second model includes the enclosure, using the Acoustic-Shell Interface, Frequency Domain to couple the structural and acoustic domains. Both 3D models

were set in COMSOL Multiphysics and have in common the basic geometry, sound source and mesh discretization.

### 3.1 General Properties

On the first hand, to model the radiating source with the absence of the enclosure, two concentric hemispheres of radius  $r_1 = 50$  cm and  $r_2 = 51$  cm were designed to represent the fluid domain (air:  $\rho_0 = 1.21$  kg/m<sup>3</sup>,  $c_0 = 343$  m/s). A Spherical Wave Radiation condition is applied on the surface of the larger hemisphere to emulate a non-reflective outer boundary condition. The inner hemisphere surface is used to derive the pressure values on its surface.

On the second hand, keeping the previous geometry, a rectangular box (32 cm x 22 cm x 26.5 cm) was centered on the plane surface of the hemispheres. The structural domain was modeled using a Shell Structural Element. This way, a Elastic Material was defined with the following properties<sup>1</sup>:  $E = 18$  GPa,  $\rho = 1089.2$  kg/m<sup>3</sup>,  $\nu = 0.29$ , and was coupled with the acoustic domain using the Acoustic-Shell Interaction interface. All enclosure's edges were fixed, except for the four ones in contact with the Hard Boundary that models the floor.

### 3.2 Sound Source

The sound source shown in Figure 1 is modelled as a Power Point Source positioned 2 mm above a sound hard sphere of 6 cm of radius and its lower extreme was positioned 2 cm above the floor. This sphere represents the geometry of the sound source used in the experimental validation. The source average sound power was measured in narrow bands according to ISO 3741 [5] and was used as an input to the models. Although the source sound power is known, it is important that the numerical model takes into account the source volume to represent its influence on the acoustical field. An illustration of the coupled acoustics-structure model is shown in Figure 3.

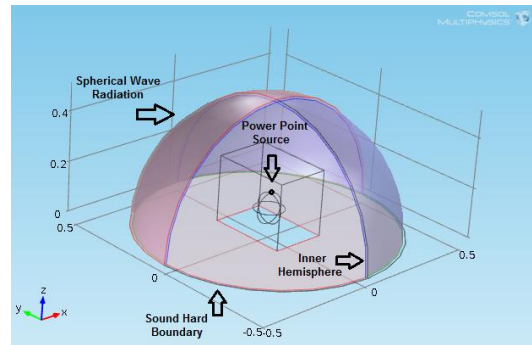


Figure 3. Coupled Acoustic-Structure Model Illustration.

### 3.3 Mesh Discretization

In acoustics, the common approach is to discretize the domain in terms of elements per wavelengths. As stated by Atalla [10], at least six elements per wavelength should be used to avoid convergence problems. The mesh elements were dimensioned in order to derive correct results up to the maximum frequency of analysis,  $f_{max} = 2$  kHz. The element size can be derived by the simple relation:

$$h = \lambda/n = \frac{c_0}{nf_{max}}, \quad (4)$$

where  $h$  is the element size, in meters,  $\lambda$  is the wavelength and  $n$  is the desired number of elements per wavelength. Thus, the mesh was built with tetrahedral elements, which dimensions respects the minimal condition to fit at least six elements per wavelength. The final mesh discretization was defined with elements of maximum size  $h = 2.8$  cm.

### 3.4 Derived Results

As the numerical model validation was intended to be done by means of IL, it is required to estimate the Average Sound Power Level ( $L_w$ ). The sound power can be calculated in terms of Sound Pressure Level ( $L_p$  dB re 20  $\mu$ Pa) [11]. The surface of the inner hemisphere with radius  $r_1$  was used to derivate the average sound pressure level, which was used to calculate the sound power level using the following simplified Equation (5):

<sup>1</sup> Where  $E$  is the Young's Modulus,  $\rho$  is the material's density and  $\nu$  is the Poisson's Ratio.

$$Lw = Lp + 10 \log_{10}(S) \text{ dB re } 10^{-12} \text{ W}, \quad (5)$$

where  $S = 2\pi r_1^2$  is the surface area of the inner hemisphere, in  $\text{m}^2$ .

The Insertion loss is the reduction of the sound power level radiated by the enclosed source, and thus, can be derived by:

$$IL = Lw_0 - Lw_E, \quad (6)$$

where  $Lw_0$  is the source power level and  $Lw_E$  is the sound power level of the enclosed source.

#### 4. Results

This Section presents the experimental and numerical results. Since the IL is derive from the sound power level, it makes sense to analyze at first moment its results. In Figure 4, one can compare the numerical and experimental results for both studied situations. The numerical results are obtained using Equation (5) and experimental results by Equation (3).

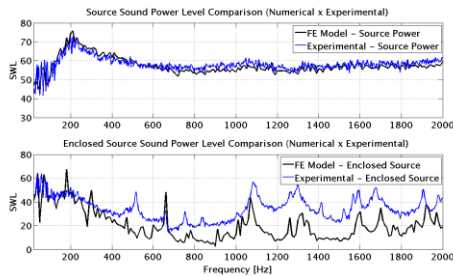


**Figure 4.** Sound Power Level Results Comparison.

It can be seen in Figure 4, that the numerical model showed very good agreement with experimental curves. Despite the fact that the numerical results for the enclosed source case have lower magnitudes than the experimental result, the curve shape is similar and predicts most of the sound power peaks. The magnitude error could be related to the boundary conditions and material properties utilized to model the structural domain. Also the sound absorption of the material is not considered as its damping factor. Hence, the structural modes of the enclosure are incorrectly estimated, interfering on the fluid-structure coupling results.

The numerical IL results are derived from Equation (6) and the experimental results are derived using the same idea, however deriving  $Lw$

values by Equation (1) and Equation (3). The results can be compared in Figure 5.

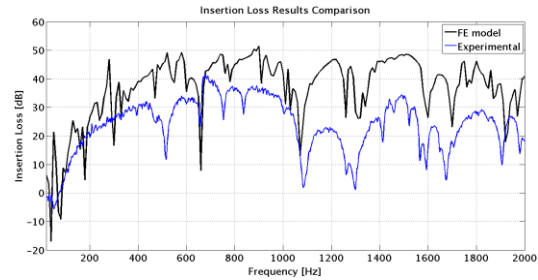


**Figure 5.** Insertion Loss Results Comparison.

Figure 5 shows that for frequencies lower than 100 Hz the enclosure is acoustic transparent, meaning that it have no attenuation effects at this range. In 660 Hz, a sudden decrease of IL is notable, meaning that the radiated noise increase and makes the enclosure a secondary source of sound pressure. The same behavior is seen in 1080 Hz, 1300 Hz and 1674 Hz, where the IL decrease is even higher and becomes almost equal to zero.

Since there is an acoustic-structural coupling between the internal cavity modes and the external radiation domain, is important to investigate the structural behavior of the enclosure. This will allow to conclude about how the structure resonances affects the IL curve. Figure 6 shows the enclosure structural displacement, which will give us an insight about the enclosure's structural modes.

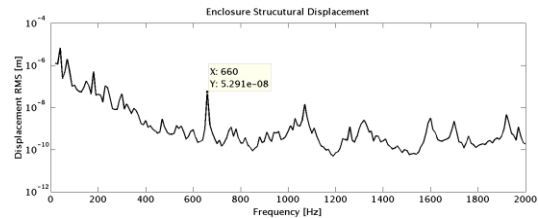


**Figure 6.** Enclosure's Structural Displacement (Surface Average).

In fact, by analyzing Figure 6, it can be seen by looking at the most prominent peak that the first mode of the structure is indeed at 660 Hz, reinforcing the hypothesis that the IL decrease at this frequency is due to a structural resonance.

By investigating the mode shapes in Figure 7 (a) and Figure 7 (b), is noticeable that bending modes occurs at 230 Hz and 300 Hz, respectively.



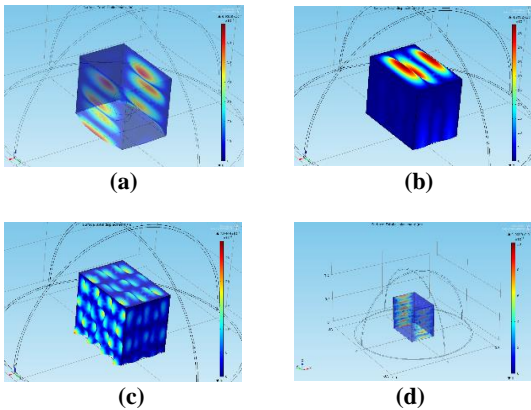


**Figure 7.** Surface Total Displacement [m] Color Plot. Structural modes: (a) 230 Hz, (b) 300 Hz, (c) 660 Hz and (d) 1080 Hz.

Figure 7 (c) shows that in 660 Hz the enclosure mode occurs in all three dimensions, thus increasing the sound radiation. Figure 7 (d) shows how the resonance structural shape occurs in 1080 Hz. Additionally, the directional pattern presented in Figure 8 and Figure 9 allows a better visualization of the directional acoustic radiation. It can be seen that the radiation is higher in the dimensions where the structural mode peaks take place. This proves that the modal resonances play a important role on the radiated acoustic field.

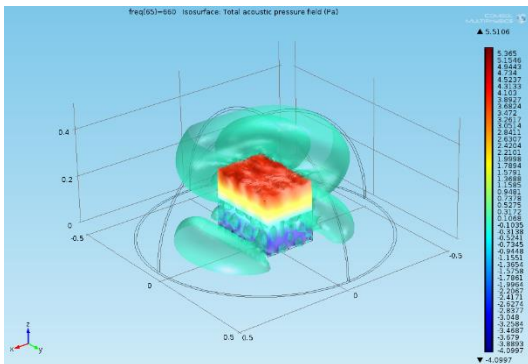


**Figure 8.** Isosurface of the Total Acoustic Field [Pa] at 660 Hz.

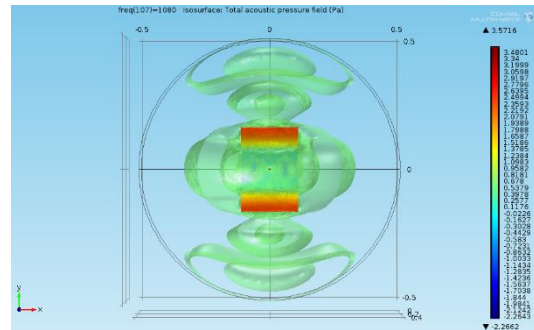


**Figure 9.** Isosurface of the Total Acoustic Field [Pa] at 1080 Hz.

## 5. Conclusions

This study validated a multiphysical model to estimate the Insertion Loss promoted by the enclosure of a sound source. The model took into account the source frequency dependent sound power, which was obtained experimentally.

The IL results exposed in Figure 3 shows that the numerical model provides a good estimate of the IL behavior. However, the improvement of this model still possible since more representative boundary conditions and material properties could lead to a better agreement between experimental and numerical IL's curves.

Notwithstanding, the investigation about the enclosure's structural behavior showed that the shell element was able to predict correctly the resonance frequencies, thus validating the FE model. This statement is supported by the fact that the IL decrease at 660 Hz (Figure 5), for both numerical and experimental cases, is in fact the first structural mode of the enclosure, as seen in Figure 6. The use of shell elements is justified especially because of the low computational cost required, in comparison to solid elements. In this case, each frequency step took around 4 minutes in a PC Core I7 processor with 16 GB RAM. Solid elements could not be evaluated because of his high RAM requirements.

Since approximated properties of the enclosure's wood was obtained from a database [12], future works shall use optimization methods to fit the numerical IL curve on the experimental IL results. This optimization would have the material properties as optimization variables. Thus, would be possible to estimate real values of material properties, which characterizes an inverse acoustic problem. At the end of that work, a reliable numerical model to estimate the IL

promoted by the enclosure of a sound source should be obtained, allowing its use as a powerful tool for enclosure design and its IL optimization.

## 6. References

1. R. F. Barron, Industrial Noise Control, CRC Press, 2002.
2. J. E. Blanks, Optimal Design of an Enclosure for a Portable Generator, Master Thesis, Virginia Tech (1997).
3. D. Oldham and S. Hillarby, The Acoustical Performance of a Small Close Fitting Enclosure, part 1: Theoretical Models. Journal of Sound and Vibration, **Volume** 150(2), 261:281 (1991).
4. G. S. Birita. Sound Insulation of a Box. PhD thesis, Technical University of Denmark, Denmark, 2007.
5. Hambric, S. and Fahnlne, J. Structural Acoustics Tutorial—Part 2: Sound—Structure Interaction. Acoustics Today, **Volume** 3(2), 9:27, (2007).
6. Sandberg, G. and Goransson, P. A symmetric finite element formulation for acoustic fluid-structure interaction analysis, Journal of Sound and Vibration, **Volume** 123(3), 507:515, (1988).
7. Everstine, G and Henderson, F. Coupled finite element/boundary element approach for fluid-structure interaction, The Journal of the Acoustical Society of America, **Volume** 87(5), 1938:1947, (1990).
8. ISO 3741:2010, Acoustics - Determination of sound power levels and sound energy levels of noise sources using sound pressure - Precision methods for reverberation test rooms, 1999.
9. F.J. Fahy, "Measurement of Acoustic Intensity Using the Cross-Spectral Density of two Microphone Signals", J. Acoust. Soc. Am., **Volume** 62, pp 1057-1059, 1977.
10. Atalla, N and Sgard, F. Finite Element and Boundary Methods in Structural Acoustics and Vibration, CRC Press, 2015.
11. Bies, David and Hansen, Colin. Engineering Noise Control: Theory and Practice, CRC Press, 2009.
12. Institutos de Pesquisas Tecnológicas, [http://www.ipt.br/informacoes\\_madeiras/38.html](http://www.ipt.br/informacoes_madeiras/38.html)